

AD 744998

HIGH ENERGY LASER WINDOWS

Semiannual Report No. 1

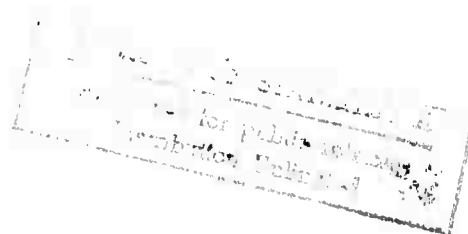
for period ending 30 June 1972

**Details of illustrations in
this document may be better
studied on microfiche**

ARPA Order 2031

**Naval Research Laboratory
Washington, D. C. 20390**

Reproduced by
**NATIONAL TECHNICAL
INFORMATION SERVICE**
U S Department of Commerce
Springfield VA 22151



**BEST
AVAILABLE COPY**

TABLE OF CONTENTS

I.	Introduction and Summary	1
II.	Crystal Preparation	3
	A. Press Forging Studies	3
	B. Chemical Polishing	22
	C. Thin Film Coatings	32
III.	Optical Absorption	36
	A. Lattice Absorption at High Frequencies	36
	B. Optical Measurements	42

I. INTRODUCTION AND SUMMARY

This report describes work done to develop an alkali halide window with suitable characteristics for laser uses.

The period covered in this report is the six months ending 30 June 1972. An earlier report for the first quarter was also distributed because of the widespread interest in this problem. As a result, this report contains material described earlier as well as more recent results.

Alkali halides have a number of attractive properties that recommend them for windows for infrared lasers. Large crystals are commercially available. The degree of chemical purity of these crystals is fairly good. In addition there has been widespread research arising from color center studies concerning ways of further reducing heavy metal impurities, oxygen, and water. It is also known that the optical absorption of some of the alkali halides in the infrared is as low as any other material. These attractive properties are balanced by others which are less attractive. The alkali halide crystals deform easily under stress and they are attacked by water.

A goal of this program is to improve the mechanical properties of the alkali halides by developing polycrystalline materials without destroying their excellent optical properties. The technique of press forging has been used because it produces polycrystalline specimens from single crystals without appreciably increasing the surface area of the material. This minimizes problems associated with adsorbed oxygen and water vapor. Press forged samples have been produced with yield stresses of 5000 to 6000 psi which is very close to the design goals and is extremely encouraging.

Polycrystalline specimens have a more complex surface than do single crystals and the preparation of a good surface is difficult. It should be optically flat, it should not introduce absorption or scattering of its own, it should be able to be produced reproducibly on samples with large areas, it should not have inclusions of foreign matter or scratches, and it should have good adhesion to protective films. Progress has been made in developing chemical polishing techniques as a final step after mechanical polishing to insure a smooth surface. A number of protective films have been tried on KCl with some success. However, the adhesion of these films is not yet reproducible. More careful preparation of the KCl substrate seems likely to be the key to a solution of this problem.

A theoretical study of the source of optical absorption has been made for alkali halides at frequencies far higher than the "Restrahl" frequencies.

The conclusions are that monovalent impurities of normal mass are unlikely to introduce serious effects. Divalent ions such as Ca^{++} and $\text{O}^=$, and light ions such as H^+ or OH^- are likely to be much more serious.

The measurement of optical absorption in low loss material has not been a simple matter even in single crystals. For polycrystalline samples the problems are aggravated by the fact that the amount of light scattered by the sample may be larger than that directly absorbed. Refinements of the measuring equipment are being developed to cope with this problem.

II. CRYSTAL PREPARATION

A. Press Forging Studies, P. F. Becher and R. W. Rice

1. Selection of Press Forging

Both the deformation and fracture of alkali halides are controlled by dislocations. Inhibiting the motion of dislocations raises their yield stress, thus making them more resistant to deformation and hence potentially much more suitable for use as high power laser windows. Dislocation motion can be inhibited by irradiation or alloying, or by obtaining polycrystalline bodies of progressively finer grain size. Polycrystalline bodies not only have higher yield stresses than single crystals, but they also have higher fracture energies which control crack growth and propagation. Irradiation or alloying often decreases fracture energies, and thus may require a trade-off between strength and fracture resistance (i. e., toughness). The polycrystalline approach was therefore selected as the primary strengthening method because it also gives higher fracture resistance. The polycrystalline approach also allows supplemental strengthening by alloying or irradiation if necessary.

Fabrication of fine polycrystalline bodies from powders (e. g. by sintering or hot pressing) was rejected because of basic problems expected in adequately removing species adsorbed on powder particle surfaces. Such species, e. g., H_2O , would be detrimental to the stringent optical requirements of laser windows. The selected approach was to develop grain boundaries in situ by plastic deformation and recrystallization of single crystals. This method completely avoids the above problem of grain boundary contamination from adsorbed species and assures void-free bodies.

The feasibility of plastic deformation and recrystallization of alkali halides was clearly established by previous studies, as exemplified in Table 1. All of the alkali halide work had been by extrusion. However, this was felt to be a less feasible and/or economical method of obtaining the end sizes and shapes desired. Rolling should be feasible (e. g., as shown by work on $AgCl$ which is more ductile), but could present problems of cracking unless the more difficult task of metal encapsulation was undertaken. Both extrusion and rolling also generally require higher temperatures and pressures because of deformation constraints inherent in the processes and the high rates of deformation normally used. Higher temperatures limit control of recrystallization and hence the extent of grain size reduction. Press forging, i. e., slow, unconstrained compressive deformation, was selected because it should be feasible at modest temperatures and pressures, thus allowing finer grain sizes and hence higher strengths to be achieved. It also

offers the practical advantage of making "short, fat" bodies from more easily grown "long, thin" crystals.

Press forging of halides was not known to have been previously studied. However, Rice (1) had utilized the technique for MgO crystals based on their high temperature deformation analagous to that of halides at comparable homologous temperatures. The technique has also been applied to polycrystalline refractory ceramic bodies (5-8) and to a variety of other refractory crystals (9). It is interesting to note that alkali halides were studied as guides to the deformation of practical refractory ceramics. Now the results of these ceramic studies are being used as a guide in practical development of alkali halide bodies.

2. Halide Bodies for Press Forging

Crystals ordered prior to the initiation of this six months' contract were not received until late in the program. Therefore much of the work was done with crystals on hand from previous halide studies. These were most commonly KCl of commercial origin (Harshaw and Optovac), but some crystals previously grown at NRL along with crystals obtained from other laboratories were used. All crystals were of good optical quality with no visible inclusions or voids (except as noted). A small ($\sim 1 \text{ in}^3$) irregularly shaped, cloudy 50% KCl-50% KBr crystal, grown several years ago, was obtained* for initial trials of press forging alloy crystals. A much larger and better quality KBr crystal, supposedly containing KCl, was also obtained.* Subsequent analysis showed that the crystal was predominantly KBr having $< 1\%$ KCl content. Additionally, a crystal of NaCl $1/2$ inch on a side by $3/4$ inch high was obtained. Both Czochralski-grown single crystals and castings of KCl (Fig. 1) were obtained from Hughes Research Laboratories**, and were indicated to be specially purified. The Hughes crystals were grown by a Czochralski technique and zone refined in an atmosphere of CCl_4 (to minimize hydroxyl content) and contained some axial tubular pores. The cast materials (Fig. 1) were rapidly solidified in vacuum, which resulted in porous, polycrystalline bodies (grain size $\sim 2-5$ mm). Strength measurements of starting crystals are shown in Table 2.

Single crystals were cleaved to approximately square cross-sectional dimensions between $1/2$ and $3/4$ inch and about twice as long as wide. Samples of about the same size were cut from the better areas of cast ingots (Fig. 1).

* Courtesy of Dr. P. Klein of NRL Central Materials Activity from earlier alkali halide crystal studies.

** Courtesy of R. C. Pastor and colleagues, Malibu, California.

All specimens were water-polished prior to forging to round surface steps and cracks that might act as sources of tearing or cracking.

3. Development of Press Forging Technique

All water-polished parallelepipeds were forged parallel with the long axis by a single top moving ram. As shown in Fig. 2, the deformation of the crystal or casting sections was unconstrained radially, and was performed in air with graphite tooling. Pyrolytic graphite tape* (0.010 in. thick) was used as a lubricant between all crystals and the graphite rams to minimize end constraints and allow more uniform deformation based on experience with refractory materials (6, 9). Radial tearing and cracking occurred in initial press forging trials by researchers at Honeywell** and Hughes*** in attempts to reproduce results of this study. They did not use such a pyrolytic graphite layer indicating that it is important.

The first two forgings were done in an induction-heated hot press with a hand-pumped hydraulic ram. A nichrome-wound furnace was then constructed in order to gain better temperature control at the modest temperatures required for alkali halides. This furnace (Fig. 2) was designed so the crystal could be dropped from the hot zone when forging was completed in order to limit recrystallization and grain growth. Forging in this furnace was then conducted using a screw-driven mechanical test machine to give a continuous, controlled motion of the moving top ram. Most forging was conducted at constant ram speeds of 2 to 5×10^{-2} in/min to achieve a constant initial strain rate of $5 \times 10^{-2} \text{ min}^{-1}$ for all forgings.

Forging at temperatures less than 125°C resulted in cracking and/or fracture of KCl using initial strain rates of $\leq 5 \times 10^{-2} \text{ min}^{-1}$ (Table 3). Cracking rapidly diminished in forgings performed at and above 125°C . The optimum temperature was about 150°C to eliminate cracking while limiting grain growth (as discussed below). Trials with higher initial strain rates (e.g., $1 \times 10^{-1} \text{ min}^{-1}$) resulted in cracking above 125°C , indicating that the $5 \times 10^{-2} \text{ min}^{-1}$ initial strain rate is about the upper limit over the optimum temperature range ($130\text{-}160^{\circ}\text{C}$). As seen in Table 4, purified KCl from Hughes forged successfully, similar to other KCl, regardless of whether it was in single crystal or large grain polycrystalline form. A typical starting KCl crystal and a section of a completed forging are shown in Fig. 3.

* Grafoil, product of Union Carbide Corporation.

** Private communication with R. J. Stokes.

*** Private communication with G. D. Robertson.

Forging trials with KBr and NaCl indicated that KBr could be successfully forged under the same, or more modest, conditions as KCl, while NaCl required temperatures of at least 300°C before a successful forging was obtained (Table 5). These results are consistent with the melting points relative to KCl. A trial forging of a 50% KCl-50% KBr body fractured at 450°C. While the poorer quality of this crystal was probably a factor, the limited ductility of such two-phase alloys is felt to be the major factor in cracking at this high temperature.

4. Characterization of Press Forged Halides

a. Grain Size and Recrystallization

Forging KCl crystals at higher temperatures (e. g., 400°C) resulted in inhomogeneous microstructures consisting of both small and large (deformed) grains. The latter often were of the order of 200 μm , and were mostly in the interior in the highest temperature forgings (Fig. 4A). Lowering forging temperatures and forging to greater reductions in height both resulted in finer and more homogeneous grain sizes as expected (Fig. 4B). Quenching followed by inert atmosphere annealing showed recrystallization and grain growth started in the 100-140°C range. Forging at temperatures of 150°C, followed by rapid cooling, gave grain sizes of about 5 μm due to suppression of recrystallization and grain growth. Annealing of these bodies resulted in some further but limited reduction of grain size. Forging at lower temperatures (i. e., <130°C) to further reduce recrystallization rapidly encountered serious cracking problems, as noted earlier.

b. Residual Strain

Polarized light examination of the forgings showed residual strain in as-forged bodies. This was also indicated by some cracking problems in machining specimens (especially in attempts to make specimens for measuring fracture energy). The degree of residual strain generally increased with decreasing forging temperatures and increasing forging reductions. Annealing at 100-140°C eliminated cracking and fracture during most subsequent specimen preparation. This indicates substantial strain relief, as does greater ductility resulting from annealing, as discussed later.

Initial Laué back reflection photos of forged specimens show extensive arcs (e. g., 20-30°), indicating substantial but not random polycrystalline character. Comparison of the height of major peaks from x-ray spectrometer data on surfaces normal and parallel to the forging direction was used to more clearly show the texture. Initial results for the KBr crystal with an 8:1 height reduction (Table 5) showed the $\langle 200 \rangle$ poles to be eight times as

intense on the surface normal to the forging direction. The $\langle 220 \rangle$ poles were in a ratio of about 4:3, no other major pole differences were found.

As noted elsewhere, optical measurements and characterization have been hindered by problems of obtaining an adequate surface finish on forged bodies. However, J. Kiefer of Hughes Research Laboratory reports absorption coefficients of the order of 0.008 to 0.03 in press forged samples of KCl supplied by them.

5. Mechanical Behavior

Test bars, approximately 0.06 in. x 0.12 in. in cross section, were wire sawn, then water-polished, for 3 point flexure testing on spans of 0.35-0.5 in. at a strain rate of $\sim 1.5 \times 10^{-1} \text{ min}^{-1}$ (i. e., a head travel speed of $\sim 5 \times 10^{-2}$ in/min). All specimens showed at least a slight yield before fracture. Yield stresses as high as 4500-5000 psi were achieved by forging single crystals (Table 4). Similar testing of the starting crystals gave yield stresses of 400-800 psi, so the stronger forged bodies are nearly an order of magnitude stronger than the starting crystals. The yield stress of forged crystals increased with decreasing grain size (Fig. 5), consistent with the Petch equation:

$$\sigma_y = \sigma_0 + KG^{-1/2} \quad (1)$$

where σ_y = yield stress, σ_0 = a constant related to the single crystal yield stress, K = a constant, and G = grain size. Forgings of fused cast material from Hughes resulted in yield stresses approaching 6000 psi.

The amount of plastic strain prior to failure of bars with as-forged structures was generally quite small (e. g. $\leq 0.01\%$). Annealing at 100°C for two hours increased this plastic strain to about $\sim 0.1\%$ (i. e., an order of magnitude increase). Fracture occurred primarily by transgranular cleavage. In bodies with mixed grain structure, fracture appeared to have initiated in the large grains. Fracture energy measurements have not yet been made because suitable samples have not been prepared.

As expected, hardness measurement (Vickers) showed limited improvement from 11-12 kg/mm^2 for starting crystals to 13-14 kg/mm^2 for forged bodies.

6. Discussion

While some second order refinement of KCl forging parameters may be needed, near optimum parameters have been determined. These have resulted in bodies with fairly uniform grain sizes of about 5 μm . Resulting

yield strengths from forged KCl crystals approaching 5000 psi have been achieved. Press forging of large grain fusion-cast KCl bodies gave yield stresses approaching 6000 psi. The higher yield stress in the latter bodies is felt to be due to more homogeneous deformation and recrystallization resulting from the presence of grain boundaries in the starting bodies. It is expected that similar results may be achieved by forging a crystal in one direction, then reforging it in an orthogonal direction.

Rapid cooling, which has been an aid in obtaining the finest grain sizes and hence highest strengths, may be of more limited use in larger bodies. Poor thermal conductivity will limit the benefits of such cooling in the central areas, and may result in serious thermal stresses in larger bodies. However, more study is necessary since, for example, cooling bodies by dropping them into an intermediate temperature zone (e. g., below the recrystallization temperature) should limit any possible thermal stress problems. As noted earlier, alloying and irradiation strengthening can be used to supplement strengthening from forging, though possible compromises between strength and fracture energy should be considered.

The strength of "Polytran" KCl, reported by Wurst (10), is in good agreement with the press forged data in Fig. 5. This questions the continuity he indicated for this Polytran strength with a branched Petch plot of earlier NaCl data of Stokes and Li (2). Use of such a branched Petch plot for halides that show macroscopic evidence of flow is also questioned, since such branched curves are most applicable to materials which exhibit only microscopic evidence of plastic flow. The NaCl data of Stokes and Li, which is equally well fitted by a single, non-zero intercept line on a Petch plot, is about the same order of strength as the present KCl data. Because of its softer nature, KCl should be somewhat weaker than NaCl. It cannot be completely resolved whether the KCl data is high or the NaCl data low, but both probably are factors. The lower strain rate, use of tensile rather than flexure testing, and the small number of grains (e. g., 3) in the gauge section of Stokes and Li's NaCl specimens, could all tend to give lower strengths than in other testing. Approximate hardness-Petch intercept, and hardness-crystal yield stress relations also indicate that these NaCl strengths are low (11, 12). These latter comparisons indicate that the KCl strengths might be somewhat high. However, this is uncertain since it is not known whether the Petch intercept for the soft halides should be equal to the single crystal yield stress (approximately so in the present study) or lower, e. g., by as much as two to three as indicated for harder materials. Clearly, much more detailed evaluation of the mechanical behavior of alkali halides is needed for more exact comparison and analysis.

While the present strength data is scattered, it lends support to a Petch analysis of strengths. In view of the indicated texture, this strength data corroborates the fact that grain misorientations of only $5-15^\circ$ are generally necessary for typical polycrystalline behavior (2). Much of the scatter is most likely due to residual strains. Further annealing studies are needed to reduce such strains and the indicated scatter. Such strain relief should also aid surface finish and optical homogeneity. The indicated texture could be due to the starting crystal orientation, deformation texturing, or recrystallization.

7. Summary and Conclusions

Press forging clearly shows excellent promise for achieving most, and possibly all, of the necessary strength for halide windows for high power lasers. While much further optical characterization is needed, no evidence shows that suitable optical properties cannot be obtained in forged halides. Strength increases with decreasing grain size are consistent with the Petch equation, and show that fully random polycrystalline bodies are not needed to achieve such behavior. Forging at low temperatures ($\sim 150^\circ\text{C}$), followed by rapid cooling to suppress recrystallization and grain growth, gave the finest grain size bodies ($\sim 5\mu$). These had yield stresses of 5000 to 6000 psi. The latter were obtained by forging of larger grain polycrystalline bodies instead of single crystals.

References

1. R. D. Carnahan, T. L. Johnston, R. J. Stokes, and C. H. Li, "Effect of Grain Size on the Deformation of Polycrystalline Silver Chloride at Various Temperatures," *Trans. AIME* 221, 45-49, 1961.
2. R. J. Stokes and C. H. Li, "Dislocations and the Strength of Polycrystalline Ceramics," in *Materials Science Research*, V. 1 (ed. by H. H. Stadelmaier and W. W. Austin), 133-57, Plenum Press, New York, 1963.
3. N. S. Stoloff, D. K. Lezius, and T. L. Johnston, "Effect of Temperature on the Deformation of KCl-KBr Alloys," *J. Appl. Phys.* 34 (11), 3315-22, 1963.
4. R. B. Day and R. J. Stokes, "Grain Boundaries and the Mechanical Behavior of Magnesium Oxide," *Materials Science Research* Vol. 3, (ed. by W. W. Kriegel and H. Palmour, III), 355-86, Plenum Press, New York, 1966.
5. R. W. Rice, "Internal Surfaces of MgO," *ibid.*, 387-423.
6. R. W. Rice, J. G. Hunt, G. I. Friedman, and J. L. Sliney, "Identifying Optimum Parameters of Hot Extrusions," Final Report for NASA Contract NAS7-276, 1968.
7. R. W. Rice, "Hot Forming Ceramics," in *Ultrafine-Grain Ceramics* (ed. by J. L. Burke, N. L. Reed, and V. Weiss), 203-49, Syracuse University Press, New York, 1970.
8. R. W. Rice, "Hot Working of Oxides," in *High Temperature Oxides* (ed. by A. Alper), Vol. 3, 235-80, Academic Press, New York, 1970.
9. R. W. Rice, "Deformation, Recrystallization, Strength, and Fracture of Press-Forged Ceramic Crystals," *J. Am. Ceram. Soc.* 55(2), 90-97, 1972.
10. J. C. Wurst, "Characterization of the Flexured Strength of Polycrystalline KCl," Report UDRI-TM-72-04, University of Dayton Research Institute, February 1972.
11. R. W. Rice, "Strength-Grain Size Effects in Ceramics," presented at the British Ceramic Society meeting on Textural Studies in Ceramics, London, December 1970, Proceedings to be published.

12. R. W. Rice, "Correlation of Hardness with Mechanical Effects in Ceramics," presented at the ASM Hardness Symposium, Detroit, Oct. 1971; Proceedings to be published.

TABLE I

MECHANICAL WORKING OF ALKALI HALIDE AND ISOMORPHOUS CRYSTALS

<u>Material</u>	<u>Technique</u>	<u>Temperature °C</u>	<u>% Tm</u>	<u>Typical Finer Grain Sizes (μm)</u>	<u>Investigator</u>
AgCl	Extruded (and cold rolled)	22 - 350	40-85	35	Carnahan, et al (1)
NaCl	Extrusion	> 300	~ 60	35	Stokes and Li (2)
KCl KCl-KBr	Extrusion	500-600	80	35	Stoloff, et al (3)
MgO	Extension	1800 (2000 anneal)	70	1000	Day and Stokes (4)
MgO	Press Forging	1850-2100	60-70	15-50	Rice et al (5, 6)
CaO	Press Forging	1600-1700	60-70	30-60 20-40 40-60	Rice et al (6-9)
MgO	Extrusion	2050-2200	80	30-300 20-100	Rice et al (6-8)
CaO	Extrusion	1700-2000	70-80	40-300	Rice et al (6-8)

TABLE 2

WATER-POLISHED SINGLE CRYSTALS

<u>Material</u>	<u>Source</u>	<u>Average Yield Stress*</u> psi	<u>Average Fracture Stress*</u> psi	<u>Average Plastic Strain</u> %
KCl	Harshaw	625	4460	~ 2
	Optovac	500	2425	~ 1
KBr - <1% KCl	NRL	582	2213	~ 1
KBr - 50% KCl	NRL	-	4285	-
NaCl	Harshaw	710	7950	~ 2

* 3 point bending, $\dot{\epsilon} = 1.5 \times 10^{-1} \text{ min}^{-1}$. The yield stress was taken as the proportional limit (zero off set), while the fracture stress was calculated from elastic beam theory neglecting the limit ductility.

TABLE 3

FORGING OF COMMERCIAL AND NRL KCl SINGLE CRYSTALS

Crystal Source	No.	Forging		Forging Results		
		Temperature °C	Height Reduction	Average Grain Size μm	Average Yield Stress [†] psi	Average Fracture Stress [†] psi
1	1*	400	3:1	15 - 200	1550	2500
1	2*	260	5:2	15 - 30	1350	3200
2	3*	25	4:3	cracked	-	-
2	4*	200	4:1 [†]	6	4350	7200
2	5*	100	3:1	12	2850	5500
2	6*	180	17:4	cracked	-	-
3	7*	160	4:1	5	3600	5800
2	8*	150	4:1	-	-	-
3	9*	150	4:1	6	-	-
3	14*	150	5:1	6	-	3000
3	15**	150	9:2	8	-	-
2	15**	150	4:1	no recrystallization	-	-

1 - Optovac

2 - Harshaw

3 - CMR, NRL

* Initial strain rate: $5 \times 10^{-2} \text{ min}^{-1}$ <100> forging axis.** Initial strain rate: $1 \times 10^{-2} \text{ min}^{-1}$.

† Tested in 3 point bending, $\dot{\epsilon} = 1.5 \times 10^{-1} \text{ min}^{-1}$. The yield stress was taken as the proportional limit (zero off set), while the fracture stress was calculated from elastic beam theory neglecting the limited ductility.

TABLE 4

FORGING OF KCl FROM HUGHES RESEARCH LABORATORY

Material	Press Forging				Results			
	Forging No.	Temperature °C	Initial Strain Rate min ⁻¹	Height Reduction Ratio	Ave. Grain Size μm	Ave. Yield Stress ¹ psi	Fracture Stress ¹ psi	Average Permanent Strain %
KCl	17	145	5×10^{-2}	4.6:1	-	(~1500)	-	-
KCl Boule 44	18	150	7×10^{-2}	4.1:1	5-7	4200	5600	< 0.01
KCl Boule 42	19	150	5×10^{-2}	4.1:1	~ 5	(~2400) 4600	- 6000	- < 0.01
same	20	150	7×10^{-2}	6.6:1	~ 5	3850	5350	< 0.01
KCl ²	21	155	7×10^{-2}	4:1	~ 5	5525	5700	< 0.01

¹ Strain rate of $1.5 \times 10^{-1} \text{ min}^{-1}$ in 3 point bending. The yield stress was taken as the proportional (i. e., zero off-set). The fracture stress was calculated from elastic beam theory, neglecting the limited ductility.

² Polycrystalline body initially with 2-5 mm grain size.

TABLE 5

FORGING OF OTHER HALIDES

Material	Forging Parameters (1)				As Forged Characteristics			
	Forging No.	Temperature °C	Initial Strain Rate min ⁻¹	Height Reduction Ratio	Interior Grain Size μm	Ave. Yield Stress psi (4)	Average Fracture Stress psi (4)	Average Permanent Strain % (4)
KCl-50 m/o KBr	10 (1)	450	5×10^{-2}	Fractured	-	-	-	-
KCl, $\leq 1\%$ KBr	11 (2)	250	5×10^{-2}	5:1	7	-	-	-
	12 (2)	200	5×10^{-2}	5:1	6	3650	4000	< 0.05
NaCl	13 (3)	150	5×10^{-2}	Fractured	-	-	-	-
	16 (3)	300	1×10^{-1}	4:1	4	3450	5600	< 0.1
KBr $\leq 1\%$ KCl	22 (2)	200	7×10^{-2}	8:1	< 5	3750	5350	< 0.02

(1) All crystals had $< 100 >$ forging axes.

(2) Crystals grown by CMRA at NRL.

(3) Crystals obtained from Harshaw.

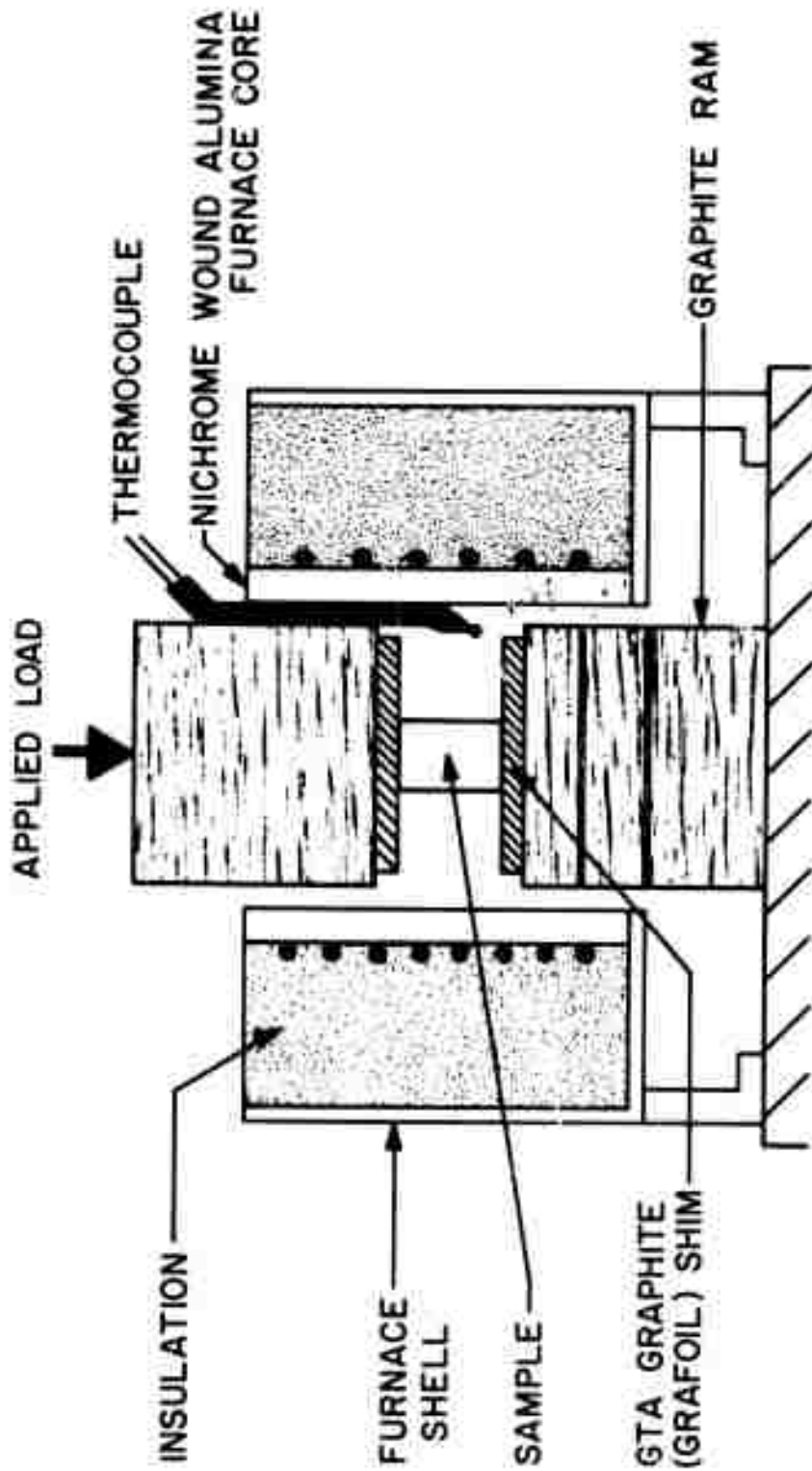
(4) Tested in 3 point bending, $\dot{\epsilon} = 1.5 \times 10^{-1} \text{ min}^{-1}$. The yield stress was taken as the proportional limit (zero off set), while the fracture stress was calculated from elastic beam theory neglecting the limit ductility.



— 4.5 cm —

Fig. 1

Ingot of vacuum cast KCl illustrating associated porosity and cracking. The clear areas near the right (tapered) end were used for forging. Grain size 2-5 mm.



SCHEMATIC OF PRESS FORGING APPARATUS

Fig. 2. The load is applied to the upper ram through the crosshead of a mechanical test machine which continuously records the applied load and resulting deflection. Note the use of end face lubricant shim and the multisection lower ram for specimen removal.



Fig. 3

KCl material before (left) and after (right) forging (forging No. 4). The height of the single crystal is $3/4$ inches, while the thickness of the forging is $\sim 3/16$ inches. The rounded edges (right) are the outer edges of the forging showing there was no edge cracking in the forging.



Fig. 4. Microstructure of Forged KCl Single Crystals.

- a. Cross section of interior of forging 1 exhibiting growth of interior grains resulting from slower cooling from 400°C in this region versus rapid surface cooling which resulted in finer grain sizes.
- b. Interior view of forging 2 illustrating uniform fine grain size as a result of rapid cooling from 260°C and residual banded structure suggesting incomplete recrystallization.

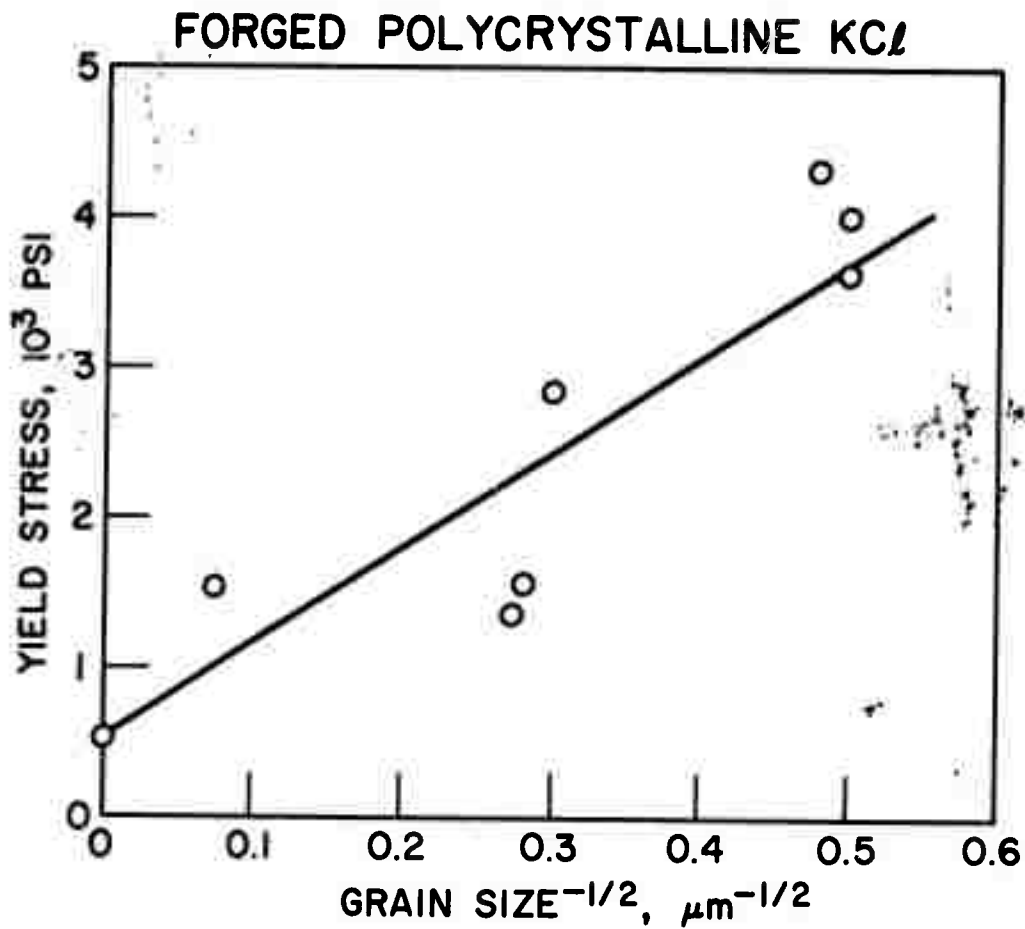


Figure 5. Petch plot for as forged KCl samples. Data points represent average yield stress values from each of several different forgings.

B. Chemical Polishing, J. W. Davisson

I. Introduction

In order to achieve successful utilization of high transmissivity hygroscopic window materials such as the alkali halides, it is essential to provide a protective coating which also might act as an anti-reflective coating as well. The performance of such coatings appears to be limited at present by the substrate surface finish which can be obtained. Since existing surface finishing techniques for alkali halides are clearly far from perfect, the development of new finishing procedures was initiated. Existing procedures leave small scratches on the surface. Since attack by water vapor is initiated at such scratches, the development of a scratch-free surface could be of considerable importance in producing substrates for subsequent coating. In the work described here, the development of chemical polishing techniques for producing high quality surface finishes on alkali halides is described.

2. Chemical Polishing

It appears that the removal of abrasive markings and scratches is a primary problem in preparing laser windows and substrates. If the surface has been rendered optically flat through mechanical action, a chemical polish will remove the scratches and leave the surface optically flat provided that the polish is a true polish. That is, provided that the polish removes existing surface layers by step migration much more rapidly than it generates new layers through generalized dissolution and provided that it does not sense individual dislocations and grain walls.

A smooth chemically polished surface on NaCl and KCl crystals is sometimes obtained when a cleavage slice of the crystal is allowed to lie quiescently in water for 30 seconds and then washed with ethyl alcohol. Such surfaces are not flat but are curved due to very rapid dissolution of the edges, and the smoothness appears to be the result of this curvature. Thus, when edge dissolution is prevented, the crystal surface frequently shows etch pits, grain walls, and roughness due to generalized dissolution. The action of the polish is improved with the addition of HCl as a buffering agent. This reduces the rate of dissolution which for NaCl can be controlled at any value between 1 - 0 microns/sec. When the dissolution rate is so reduced the removal of surface layers by step migration is more likely and a smooth surface is more likely to result. For (100) surfaces of NaCl and KCl crystals the best polishing action was obtained with the HCl/H₂O volume ratios of 3/1 and 1/0 respectively. The surface to be polished was held vertically, agitated in the polishing solution 30 sec. ,

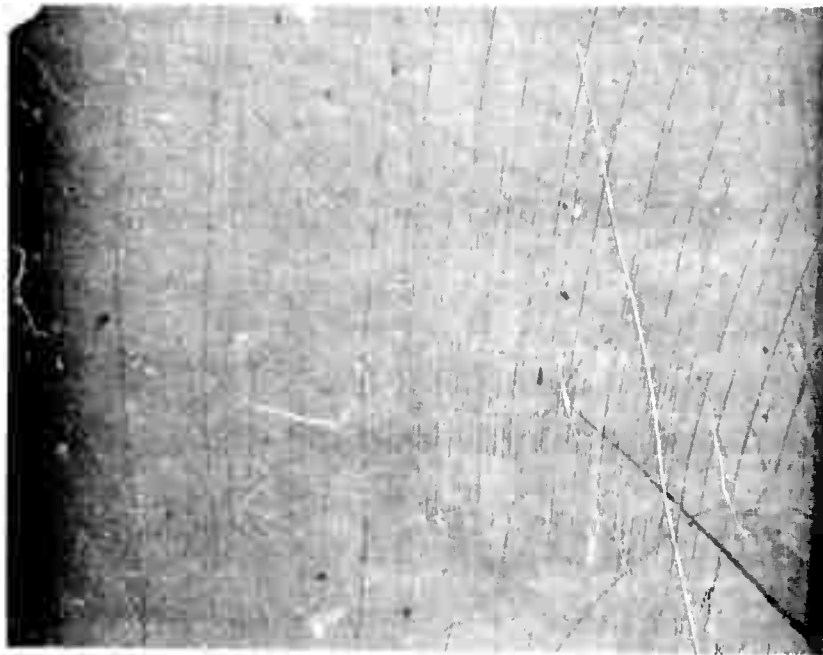
and then immediately washed with a jet of ethyl alcohol. The removal of the alcohol from the surface is sometimes a problem, since "water marks" tend to form if drops remain on the surface.

Let us now examine the action of the polish on (100) surfaces of NaCl and KCl crystals. The action on a cleavage face of NaCl is shown in Fig. 1. Although the polished surface in this case shows some roughness which might be due to incomplete removal of the polish, the important things to note are first the removal of the accidental surface scratches and the removal of all but the largest cleavage steps; and, second, the absence of dislocation etch pits and grain walls. Thus on this surface a true polishing action has been achieved. For the subsequent studies, the surfaces of the NaCl crystals were first mechanically treated either by mechanically polishing or by lapping or by both, (Fig. 2). Figure 3 shows the removal of surface scratches by chemically polishing a mechanically polished (cf. Fig. 2) cleavage face of NaCl. Figure 4 pertains to a chemically polished surface of NaCl obtained after lapping. The left view shows the chemically polished surface and the right view shows that the excessive surface dislocation damage introduced by lapping can be removed by prolonged polishing. Thus after 10 min. of polishing the etched chemically polished surface showed a normal background of resolved dislocations which implies the virtual elimination of the surface damage.

In general, the surfaces obtained by chemically polishing KCl crystals have not been as smooth as those obtained with NaCl, but this might be due to lack of experience. There is sometimes a tendency for the surface to become pocked with shallow depressions, which might be associated with non-uniform stress introduced by mechanically working the soft crystal. This seems plausible because smooth surfaces are readily obtained by chemically polishing fresh cleavage faces of KCl and by polishing annealed press-forged KCl crystals. If so, then the polishing action would be better in annealed crystals. Figure 5 shows a smooth surface that was obtained by chemically polishing a KCl crystal that had received a fine mechanical polish, and Fig. 6 shows remarkably smooth chemically polished surfaces of annealed press-forged KCl. Figure 7 shows interferograms of some of our chemically polished surfaces taken with a Zeiss interference microscope at 10X objective magnification.

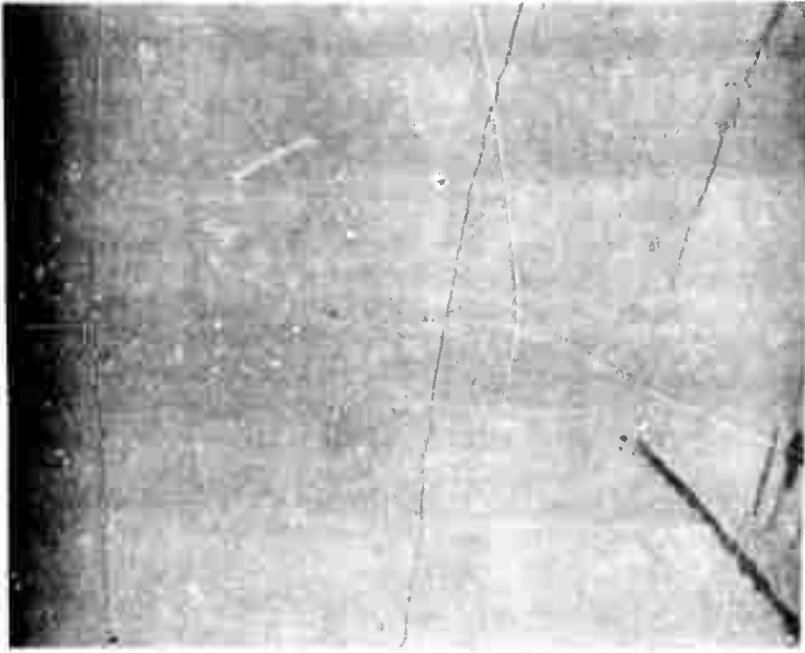
Although the surfaces are smooth, the chemical polish as presently developed degrades to some extent the degree of flatness that is achieved with a mechanical polish. Thus the interferograms of Fig. 7, though typical, do not represent the condition of the whole surface. When the surface is scanned, the interference pattern shows distortions and changes. A flat chemically polished surface might be obtained by combining the actions of mechanical and chemical polishing into a single operation.

It should be mentioned that the optical transmission of NaCl crystals in the range from 3 to 20 microns was the same for chemically polished and mechanically polished specimens. Both were transparent out to 12 microns as measured on an ordinary infrared spectrometer.



Before chemically polishing

Reproduced from
best available copy.



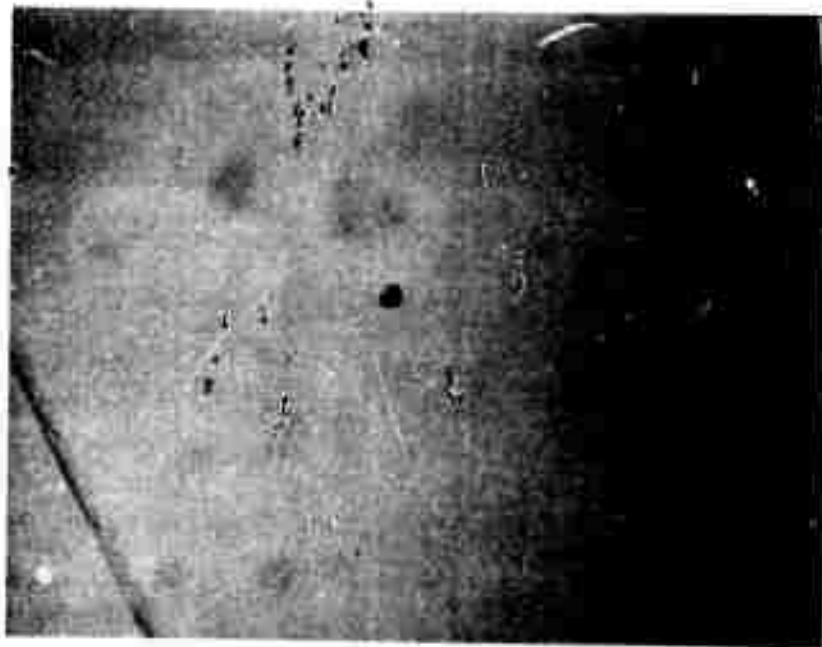
After chemically polishing

Figure 1 - Cleavage face of NaCl (X 50).



Reproduced from
best available copy.

Figure 2 - Rough mechanical polish (X 50).




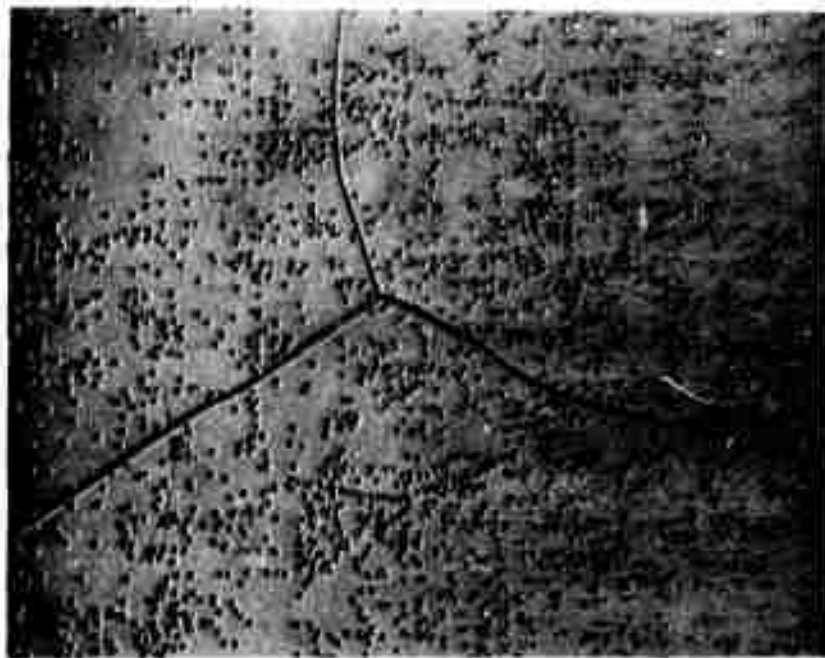
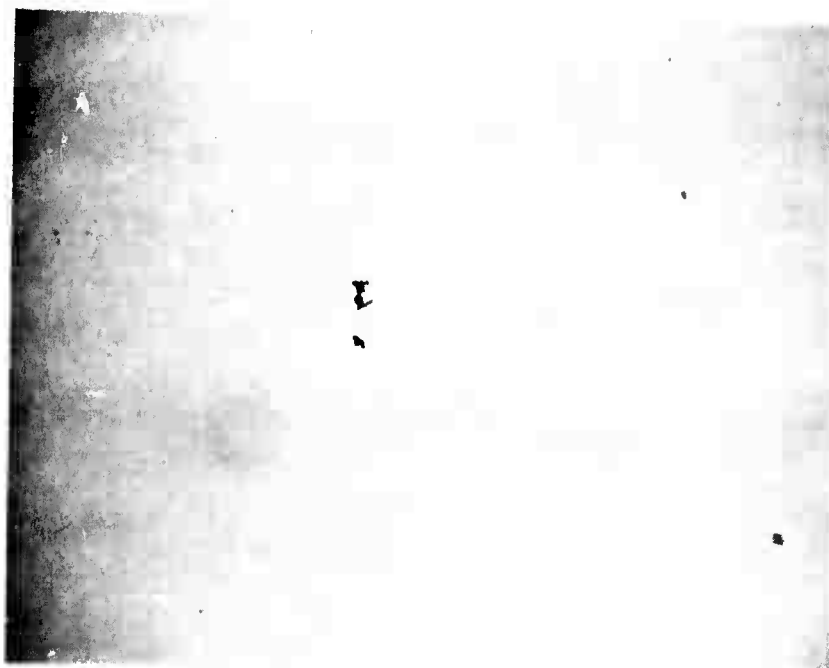
Reproduced from
best available copy. 

Figure 3 - Chemically polished, abraided
cleavage face of NaCl (X 470).



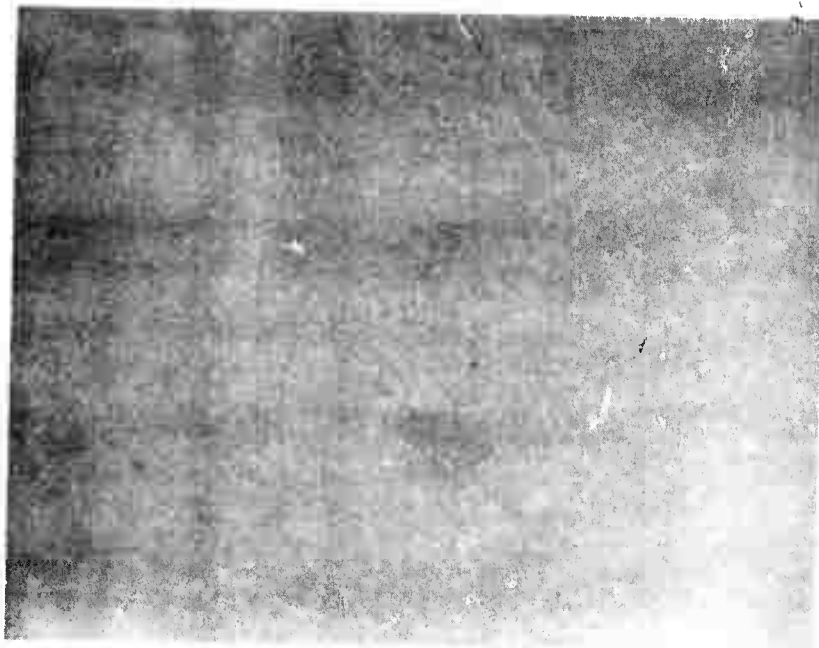
Reproduced from
best available copy.



30 Sec. Polish (X 45)

Etched after 10 min. polish (X 470).

Figure 4 - Chemically polished, lapped NaCl crystal.



Reproduced from
best available copy.

Figure 5 - Chemically polished, lapped and
mechanically polished KCl crystal
(X 200)

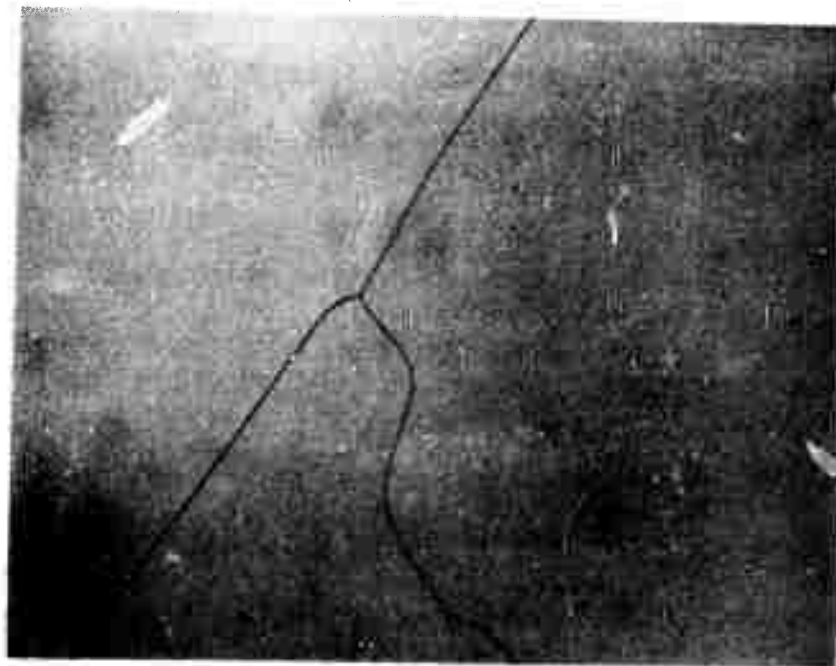
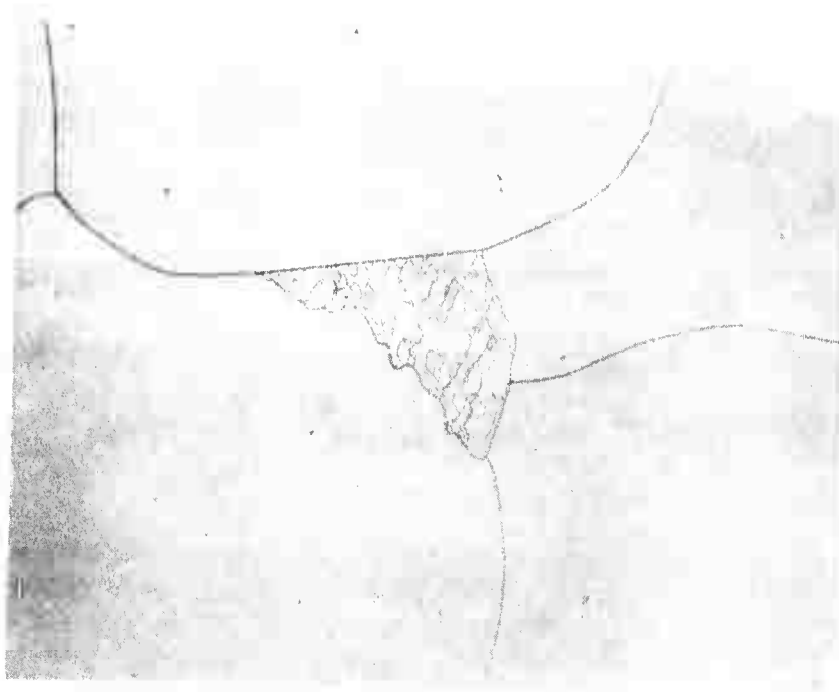


Figure 6 - Chemically polished, press-forged KCl (X 200).

Reproduced from
best available copy.



Reproduced from
best available copy.

Figure 7 - Interferograms of chemically polished surfaces

Left: NaCl Fig. 4

Middle: KCl Fig. 5

Right: KCl Fig. 6

1. Background

In conjunction with the laser window project, thin film investigations have been undertaken for possible protective coatings for KCl. Two major requirements of the film materials are, first, that they not absorb at 10.6μ and, second, that they be adherent to the window and protect it against water damage. Though p-type crystalline Ge, GaAs, and GaP exhibit free carrier absorption at 10.6μ , amorphous films of the same materials may not have the same bond structure and may not absorb at 10.6μ . Thermal mismatch of the substrate and films should not be important if the depositions are done at room temperature, though careful preparation of the substrate materials is extremely important particularly because of their softness and water solubility.

2. Progress

We are able to deposit either elemental or compound semiconductors by molecular beam deposition. In the case of the latter, the deposition is by co-evaporation of the elements. In such a deposition system it is mandatory to transfer the volatile element by multiple collision with the heated walls of the deposition chamber. The chamber is usually held at about 150°C to insure transfer. This temperature, in the standard system, is the minimum temperature at which the films are deposited. It was found that the thick films (20μ) deposited on KCl resulted in a deformation of the substrate due to thermal expansion mismatch. The deposition systems had to be modified such that the actual deposition zone (the substrate) could be held at room temperature while the transfer of the volatile component could be done at elevated temperature. The modifications have been made and many successful depositions of GaP and GaAs on KCl carried out in the thickness range from 0.3 to 20μ with no strain effects observed.

In some cases, however, GaAs, GaP, and Ge thin films have cracked along 110 directions on KCl substrates very quickly upon removal from the vacuum system. This is a problem of substrate preparation and handling and perhaps water damage because the problem does not arise when films are deposited under identical deposition conditions on glass, quartz, or sapphire substrates for which polishing and cleaning techniques are well developed.

While thin films ($\sim 0.3\mu$) are expected to be utilized in the actual coating of the KCl windows, the low absorption at 10.6μ precluded meaningful optical absorption measurements. Thus, depositions, for thick-

nesses up to 20μ were carried out where it was expected that interference effects would be minimal. These thick films were evaluated by conventional techniques and results will be given below.

As mentioned above, films of about $1/4 \lambda$ are expected to be used as the coatings. Thus, while carrying out the thick film measurements, a parallel set of measurements are being performed using calorimetric techniques. Films of Ge, GaAs and GaP have been deposited on KCl and NaCl for this purpose and are now being evaluated.

It is emphasized that to adequately characterize these films for use at 10.6μ , in the thickness range required, careful measurements of the index of refraction and its reproducibility must be included in this program. Such measurements have been undertaken.

3. Results

Substrate preparation techniques are very important, and significant improvements have been made in cooperation with Codes 5205, 6060, and 6460. The softness and water solubility of the alkali halides make it quite difficult to obtain large, optically flat, scratch-free, clean surfaces. Considerable improvement has been made in mechanical polishing procedures, and chemical polishing used quite advantageously with NaCl is now being developed for KCl. Briefly, for NaCl a 15 - 30 sec. agitation of a mechanically well polished crystal in a solution of 3 parts HCl and 1 part H_2O yields surfaces which are quite flat and scratch-free. As yet the technique is not as successful with KCl which tends to etch rather than polish. For KCl concentrated HCl is used due to its higher water solubility.

Annealing of the samples prior to mechanical polishing may be necessary. In this way residual stress, which may be the cause of the films' cracking, can be relieved.

Thin films of GaAs, GaP, and Ge have now been prepared for absorption measurements by the calorimetric technique. Two films of different thickness and an uncoated substrate, the three substrates all having the same polishing history and same thickness are being used in the film evaluation for each material.

Optical absorption measurements of thick germanium, GaAs, and GaP films also have been made. In particular these included two GaP films deposited at the same time, two GaP films deposited on KBr, one of which was thin ($\sim 3000 \text{ \AA}$), one free floating GaP thin film, four GaAs films deposited at different times one of which was deposited on KBr

rather than KCl, and two germanium films deposited at different times one of which was free floating and thin ($\sim 3000 \text{ \AA}$).

The absorption of the thick films at 10.6μ is outlined in the table below. It should be noted that in the case of the GaAs films the optical spectra were not consistent from film to film though in two cases the film thicknesses were nearly identical. The spectra for the GaP films deposited at the same time were essentially identical.

<u>Material</u>	<u>α (cm^{-1}) at $10.6\mu\text{m}$</u>	<u>d (μm)</u>
GaAs on KBr*	1.9×10^3	11.0
GaAs	6.5×10^2	24.5
GaAs	2.4×10^2	24.4
GaP	2.5×10^2	21.2
GaP	2.6×10^2	20.2
Ge	4.8×10^2	15.5

* Films deposited on KCl unless noted.

The absorption coefficient of the thin films at 10.6μ was difficult to ascertain reliably because of the small absorption and the interference fringes.

The GaAs film with the intermediate α at 10.6μ listed above showed distinct intravalence absorption at energies further out in the infrared though the film with the lowest α did not. One additional GaAs film which was apparently stressed because it was deposited at a higher temperature than the others showed very high absorption nearer the visible, possibly due to the split-off valence band and decreasing absorption from about 0.27 to 0.05 eV. This last film is not listed in the table above as it was destroyed in attempting to float it off the substrate before the thickness was measured; however, α was higher than the other GaAs films at 10.6μ if the deposition rates were nearly the same.

Deposition rates are quite well controlled for all the films. The GaAs results indicate, however, that other deposition parameters were not the same for thick films deposited at different times, and these conditions must

be brought under control. In addition, the high α values may or may not be limiting factors of the films, though it would be desirable to deposit films with considerably lower absorption.

III. OPTICAL ABSORPTION

A. Lattice Absorption at High Frequencies, Herbert B. Rosenstock

Let us first consider molecular or lattice absorption by a single vibrational quantum, i. e., the harmonic approximation. The intensity of absorption is then known to be determined by the square of the matrix element of the dipole moment. This absorption occurs at the frequency of the vibration itself (or, quantum mechanically speaking at the frequency $\omega = E/\hbar$, where E is the energy of the oscillator). At other frequencies the absorption is 0. The above is true for both molecules and for solids, which are simply considered to be large molecules. One would expect a difference between solids and molecules to arise from the quasicontinuous density of vibrations in the former, compared to the few discrete vibrations in the latter. In fact, this is not found, on account of the fact that for the vast majority of vibrational modes in a solid the dipole moment vanishes for symmetry reasons. Thus, in a solid as well as in a small molecule, the vibrational absorption spectrum in the harmonic approximation consists of very few lines only (often only one line, the "restrahl" absorption) occurring at or near the highest of all the vibrational frequencies. Deviations from perfect symmetry, as caused by impurities, or even surfaces, provide other vibrations with a finite dipole moment and thus the possibility of first order absorption at those frequencies.

Absorption at frequencies higher than those of lattice phonons must arise from a mechanism more complicated than harmonic ("single phonon") absorption. Anharmonicity in the lattice provides such a mechanism; it causes interaction between the various phonons that, in the harmonic approximation, are wholly independent of each other. A vastly more complicated absorption spectrum can now be expected, since all combinations of two phonons, or three phonons, or more, can now produce absorption. I. e., absorption might occur at any frequency $\omega = (E_1 + E_2)/\hbar$, or $(E_1 + E_2 + E_3)/\hbar$, etc. may arise from phonons or respective energies E_1, E_2, E_3 , etc. However, one limitation persists from the harmonic approximation: It takes a mode with a nonvanishing dipole moment to couple to the incoming light in the first place. Thus, in the examples above, one of the two phonons E_1 or E_2 , or one of the three phonons E_1, E_2 , or E_3 , must have a nonvanishing dipole moment, or, in case of the ideal crystal, must be the "restrahl" or "dispersion oscillator". In case of a defective crystal - one that contains impurities, vacancies, dislocations, surfaces, etc. - any mode with a finite nonvanishing dipole moment can take the place of the dispersion oscillator in coupling to the incoming light.

The dipole moment of the lattice is thus of importance both for the harmonic (single phonon) and highly anharmonic (multi-phonon) absorption, but in a different way. In the former case, to find the intensity of absorption at any specific frequency ω_1 , we need to know the dipole moment, if any, of a vibration having the precise energy $E_1 = \hbar \omega_1$. In the latter, absorption at some frequency ω_k can be provided by a large number of combinations of different phonons $E_1 \pm E_2 \pm \dots \pm E_j$ provided only that $\sum_j \pm E_j / \hbar = \omega_k$, and its intensity will be related to the nonvanishing dipole moment of any one of the E_j . In other words, any phonon with a nonvanishing dipole moment regardless of its energy is able to couple to the incoming light of any frequency and initiate the phonon absorption process. The absorption at this, or any other frequency, will then be roughly proportional to the square of the total dipole moment of all the phonon in the lattice. Thus, the quantity of interest for the multiple phonon absorption is the sum of the squared dipole moments of all the phonons. Before we proceed to study this quantity, we should eliminate one possible point of confusion. Since we have already seen that impurities or irregularities provide finite dipole moments at frequencies where there were none in a "pure" lattice, can we not conclude at once that the sum of the squares of all the dipole moments will always increase with impurity concentration? We cannot, for an accompanying effect might be a decrease in the dipole moment of the main absorption. We should therefore study the sum of the square dipole moments ab initio.

It turns out that a simple expression for the sum of the squares of the dipole moments of all modes can be obtained under rather general conditions. The dipole moment of a mode is defined as¹

$$P_j = \sum_l e_l x_{lj}$$

where l labels the atoms, j the modes, x_{lj} is the displacement of the l th atoms when the j th mode is excited, and e_l the charge on the l th atom. If we deal entirely with monovalent atoms, this becomes

$$P_j = e \sum_l (-)^l x_{lj} \quad (1)$$

For crystals in more than one dimension, this expression is somewhat more complicated,

$$P_j(\theta) = e \sum_l \sum_{\alpha=1}^3 (-)^l x_{lj}^{\alpha} \cos(\theta, \alpha) \quad (1.5)$$

viz. to compute the dipole moment for light in the θ direction each atomic displacement (which may be in direction x, y, z , or $\alpha = 1, 2, 3$) must be

modified by the appropriate direction cosine. Our interest will be in evaluating

$$\Pi^2 = \sum_j p_j^2 \quad (2)$$

the total sum of the squares of dipole moments of all modes.

To evaluate (1), we need the normal mode coordinates. These are defined by two expressions for the kinetic and potential energy,

$$T = \frac{1}{2} \sum_l m_l \dot{x}_l^2, \quad V = \frac{1}{2} \sum_l \sum_{l'} \alpha_{ll'} x_l x_{l'} \quad (3)$$

and

$$T = \frac{1}{2} \sum_j \dot{q}_j^2, \quad V = \frac{1}{2} \sum_j \omega_j^2 q_j^2 \quad (4)$$

Here x_l is the displacement of the l th atom, the q_j are the normal mode coordinates, m_l is the mass of the l th atom, and ω_j the frequency of vibration of the j th mode (as is verified by writing down the Lagrangian equations of motion for the expression (4)). A transformation

$$m_l x_l = \sum_j s_{lj} q_j \quad (5)$$

that carries (3) into (4) is known to always exist.² A number of properties of the transformation coefficients s_{lj} , sufficient to evaluate (2) can now be obtained by some purely formal calculations without specifying the nature of the system in any more detail.

First put (5) into (3a) and exchange the order of the sums; we then find that (4a) results only if

$$\sum_l s_{lj} s_{lj'} / m_l = \delta_{jj'} \quad (6)$$

Next, multiply (5) by s_{lj} / m_l , sum over l and use (6) to obtain

$$q_j = \sum_l s_{lj} x_l \quad (7)$$

the inverse transformation of (5). Finally, put (7) into (4a), exchange order of sums, and find that (3a) results only if

$$\sum_j s_{lj} s_{l'j} = m_l \delta_{ll'} \quad (8)$$

x_j , defined in (1) as the displacement of the l th atom in the j th mode, is from (5), S_{lj} / m_l . Thus

$$\rho_j^2 = e^2 \sum_l (-)^l (S_{lj} / m_l) \sum_{l'} (-)^{l'} (S_{l'j} / m_{l'}) \quad (8.5)$$

and, summing over j , (2) becomes

$$\pi^2 = e^2 \sum_l \sum_{l'} \frac{(-)^{l+l'}}{m_l m_{l'}} \sum_j S_{lj} S_{l'j}$$

or with (8)

$$\pi^2 = e^2 \sum_{l=1}^N 1/m_l \quad (9)$$

the sum being taken over all atoms in the crystal. This then is the quantity to which absorption at high frequency, well beyond those of any individual phonon, is roughly proportional. For a monatomic crystal, this becomes even simpler, $N e^2 / m$; but let us keep things more general than that. Indeed, let us look at what assumptions we have made to obtain (9), and which not.

1) Most importantly, we have not said that we are dealing with a perfect crystal or one with "cyclic" boundary conditions or one without impurities or other defects, nor have we specified long or short range forces in any way, nor even said anything about the order in the lattice.

2) We did however specify that each atom has the same charge, and

3) We did specify that the crystal was one-dimensional. Of these three points, the third is the most troublesome. It can be partly waved away by averaging (2) with (1.5) over the incidence angle θ , (on the theory that real solids consist of randomly oriented microcrystallites). Then, as

$$\int d\Omega \cos(\alpha, \theta) \cos(\beta, \theta) = \delta_{\alpha\beta} \quad , \text{ we see that the only effect in}$$

(8.5) would be removal of some of the terms in the series (to wit, 2/3 of the terms would be omitted). One might think this should not have a gross qualitative effect on the result (9), but one cannot be sure.

The main point is the apparent simplicity of (9) in spite of the generality of the model implied by 1). One consequence is that no effect would be expected at all from changes in the surface conditions, provided only that the total number of atoms is unchanged. Another is that only very small changes would result from one substitutional monovalent impurity, of reasonable mass, as only one of the many terms in the sum (9) would be affected. With N the total number of atoms (or of terms in (9)), a fractional

change of order $1/N$ in the absorption would result from one substitutional impurity, and a change of order $c = n/N$ from such n impurities. That is, with an impurity concentration c , the absorption should be

$$\pi^2(c) = \pi^2(c)[1 + \gamma c]$$
 with γ a constant of order unity. An exception

arises when the impurity mass in (9) is very small; then (9) changes greatly. Formally, this could arise if an atom were replaced by an electron. In that case, the preceding treatment should of course be replaced by a more sophisticated quantum mechanical one, although surprisingly accurate qualitative results have in one case been obtained by such simple-minded treatment of color centers.³

The analysis has concentrated on multiple phonon absorption where any single phonon was much smaller than the energy of the incident photon. This would be the case for substitutional monovalent ions of ordinary mass. The analysis does not apply to cases where the phonon energy approaches the photon energy and single or two phonon absorption can occur. Such cases might be expected for divalent ions of small mass such as Ca^{++} or O^- . Monovalent ions like H^+ or the ubiquitous OH^- might also be expected to cause trouble.

This analysis would suggest that the principal absorption at 10.6μ is likely to arise from such high energy phonon systems.

References

1. The classical expression (charge times displacement, summed over all atoms) and the quantum mechanical one (matrix element of the displacement vector, summed over all atoms) can be shown to be equivalent, except for very small crystals. H. B. Rosenstock, J. Chem. Phys. 27, 1194 (1957).
2. C. Jordan, Comptes Rendus 74, 1395 (1872).
3. H. B. Rosenstock and C. C. Klick, Phys. Rev. 119, 1198 (1960).

B. Optical Measurements, M. Hass and F. W. Patten

Since the effort in this program has been oriented towards the determination of the properties of press-forged materials, we have devoted a considerable amount of time to the development of techniques suitable for the measurement of the absorption coefficient at 10.6 micrometers in highly scattering materials. While the scattering at 10.6 microns is expected to be considerably less than that observed in the visible region (using a He-Ne laser), it can be a considerable problem in the measurement process. As a result, care must be exercised in the selection of the appropriate technique. During the past few months, we have evaluated various methods of measurement.

Several methods have been described for the calorimetric determination of absorption coefficient. Most investigators have chosen to measure the temperature change of a thermally isolated sample on irradiation with a laser beam. This shall be denoted as the "adiabatic" method, although the term is not strictly correct in all cases. An alternative method, designated as the "substitutional" method involves connecting the sample through a conducting post to an isothermal bath. The temperature differential conducting post on laser irradiation is measured and the absorbed power is determined by passing current through a resistor located near the temperature sensor to produce the same temperature increase. The two methods are illustrated schematically in Fig. 1.

The assumptions underlying these approaches have not always been fully appreciated and this can lead to some inaccuracy in the resultant absorption coefficient. We shall discuss the substitutional method first. The important assumption involved in the substitutional method is the equivalence of laser heating and electrical heating. There are two major failings in this particular assumption. In the first place the laser beam can scatter radiation to the conducting post, this radiation can be absorbed and provide a false reading. Scattering can be either internal or at the surfaces. Secondly, unless the substitutional resistor is located in the same position as the path of the laser beam, heat loss mechanisms can be important. Since it is physically impossible to satisfy the location condition, the validity of this assumption should and can be checked. More explicitly, the major heat loss mechanisms are conduction through the post, convection, and radiation. It would be desirable to arrange it so that thermal conduction through the post is the dominant heat loss mechanism. This assumption can be checked easily by placing another substitutional heater on the sample and checking to see that the resistor on the sample and the resistor on the conducting post give the same results.

During the early phases of this work, we found that this condition was not satisfied by perhaps a factor of two. We were able to improve the situation in two ways. First of all, the conductivity of the post was increased to match approximately that of the alkali halide sample. Second, the vacuum was improved so that convection was no longer a heat loss mechanism. In this way, substitutional heating at a resistor attached to the sample or on the conducting post agreed to within 10%. With further work, we probably could have improved this even further.

While the substitutional method need not require vacuum conditions, we found it necessary to employ a vacuum and also feel that an experimental check in the manner indicated is necessary to be certain. Since this method depends upon the thermal conductivity of the sample, materials such as GaAs and Ge having a higher thermal conductivity might be measured more easily than KCl.

After improving the system to the stage where the power absorption measurement was largely independent of the sample characteristics, we proceeded to study the absorption of various samples using the CO₂ laser as the heat source. Here it was evident that scattered radiation from the windows introduced some small errors. While these could be accounted for, it was apparent that scattering by the sample itself might introduce more serious errors which could not readily be accounted for. Since press forged materials would be apt to scatter even more, it was decided to try a different approach which might be more suitable. Thus, the main difficulty is that in the substitutional method the sample rests on a small platform to provide a thermal link; this entire platform can in effect behave as a large area infrared detector, and consequently this method has an inherent difficulty with samples which contain some scattering centers.

In order to reduce the detecting area, the alternate method involving the "adiabatic" method was attempted. In this approach, the thermal sensor can be a thermocouple having a small area. Most investigators using this approach have measured the rate of change of temperature on laser irradiation. To a first approximation this is a constant (the details are covered in the Appendix). Major problems encountered with this method have been the attachment of the thermocouple to the sample. In most cases this has been clamped or cemented to the sample surface. We have chosen to place the thermocouple into a hole drilled into the sample. The resulting thermal emfs, of the order of microvolts, can be measured readily and the stability of the system provides one indication of good thermal linkage.

At present we have measured several samples in this way, but have encountered a few problems. In the first place, some reproducibility

problems have been encountered which we believe are due to corrosion of the thermocouples by the alkali halide. Presumably this problem can be solved. Secondly, some variations in apparent absorption coefficient of about a factor of three have been observed, depending upon the placement of the thermocouple with respect to the beam. The origin of this variation is uncertain.

While we feel that the adiabatic method or some variation of it is most suitable for low absorbing materials which scatter, there are still some improvements and variations that we would like to try. A further refinement might be some hybrid measurement method combining the best features of the adiabatic and substitutional methods. That is, it should be possible to implant a small resistor inside a sample to measure the heating rate from an electrical source. This effectively measures the heat capacity of the sample and thus provides a comparison of the heat absorbed in terms of an electrical standard.

In this way, it would be possible to check the validity of the adiabatic method which has such widespread application. While this should not indicate any great discrepancy with respect to existing results in optically clear crystals, we feel that such a comparison is of even greater importance in crystals having scattering centers. Probably the biggest source of error is absorption of scattered radiation by the temperature sensor. While thermocouple sensors are small, the coupling attachment of the thermocouple to the crystal is large. While the present graphical results suggest that this method is satisfactory, it would be desirable to have an independent check of the results.

APPENDIX I

"Adiabatic" Measurements

The measuring method employed by us is similar to that described elsewhere. The technique consists of heating a sample in a laser beam and measuring the temperature time curve. A typical experimental curve is shown in Fig. 2. The sample is initially at a constant temperature. On heating with a laser beam, (in our case a Sylvania Model 941 measuring about one watt after passing through the sample), a small discontinuity is sometimes observed which has been attributed to scattering by the laser beam. The temperature then rises, eventually giving a constant slope after quasi-equilibrium conditions are established. On blocking the laser beam, a small discontinuity may be observable followed by a cooling curve. In air this would be primarily due to convection. In a good vacuum, radiation is probably the dominant loss mechanism, with conduction through sample supports and thermocouple leads also contributing. Our samples are supported by pointed nylon rods. Copper-constantan thermocouples of 5 mil diameter have been employed so far. As indicated by the group at AFCRL, measurements can be conducted in air for rapid measurement, and we have found this convenient also.

The differential equation describing the system can be approximated in the following way:

$$mc \frac{dT_1}{dt} + \sigma \epsilon A (T_1^4 - T_0^4) + \gamma (T_1 - T_0) = \beta_A L P_{inc} \quad (1)$$

where

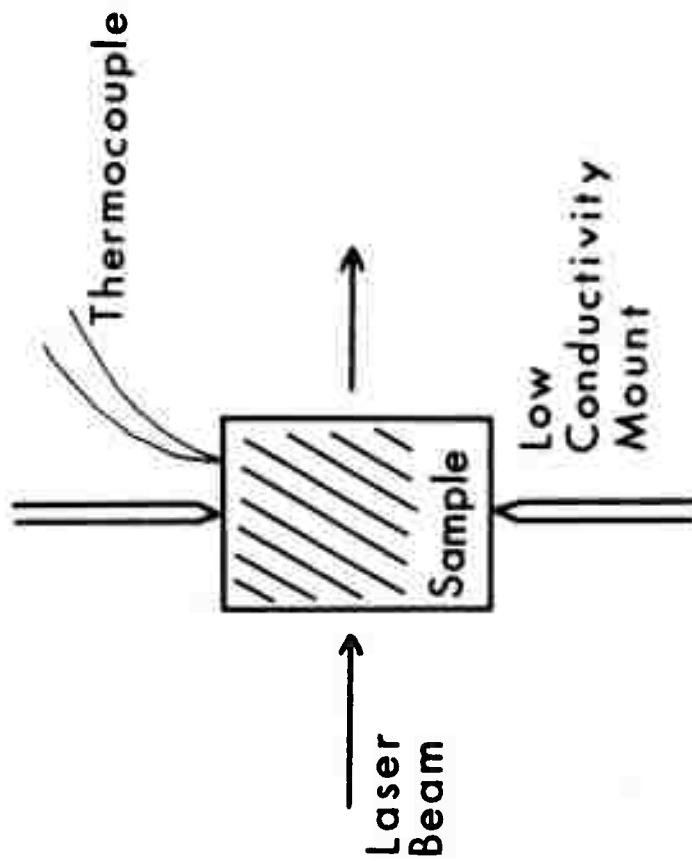
- m = mass
- T_1, T_0 = sample and ambient temperature
- t = time
- ϵ = emissivity
- σ = Stefan Boltzmann constant
- A = sample area
- γ = thermal conduction and convectors
- β_A = absorption coefficient
- L = sample length
- P_{inc} = incident power

Since $T_1 - T_0 \ll T_0$, it is possible to simplify Eq. (1) so that it can be rewritten as

$$mc \frac{dT}{dt} + K(T_1 - T_0) = \beta_A L P_{inc} \quad (2)$$

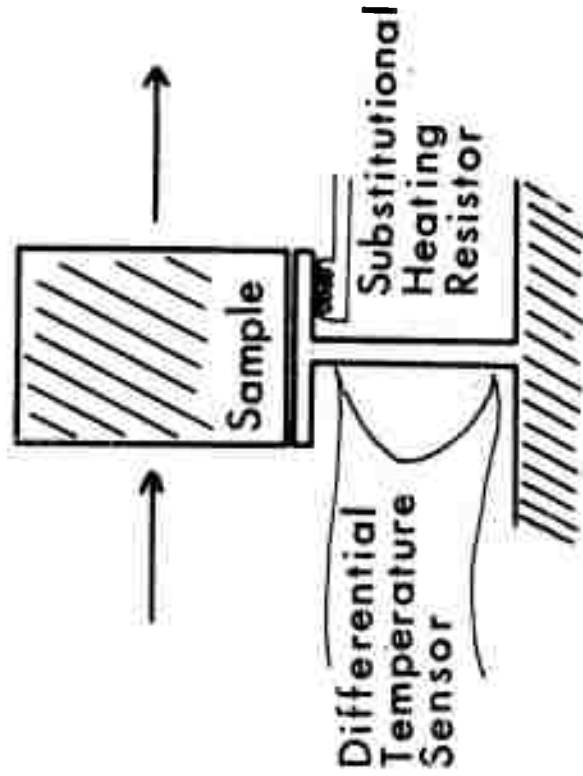
in which K includes conduction, convection, and radiation effects. This differential equation contains two unknowns, β_A and K. If the second term (2) is small compared to the first, Eq. (2) predicts a linear temperature rise after a short time, and this is observed. As the sample temperature T_1 increases, a departure from linearity is observed due to contributions from the second term. If the laser is turned off, the sample cools exponentially and the constant K can be evaluated. An easy way of doing this is by obtaining the initial slope for cooling so that Eq. (2) can be employed with P_{inc} set equal to zero. Having evaluated K, it is trivial to obtain β_A from Eq. (2).

In our experimental work, we have employed a one watt laser and have easily measured thermal emfs in the microvolt region using a Keithley Model 149 microvoltmeter. This corresponds to temperature rises of about several tenths of a degree.



a

Fig. 1(a) "Adiabetic" method for determining absorption coefficient.



b

Fig. 1(b) "Substitutional" method for determining absorption coefficient.

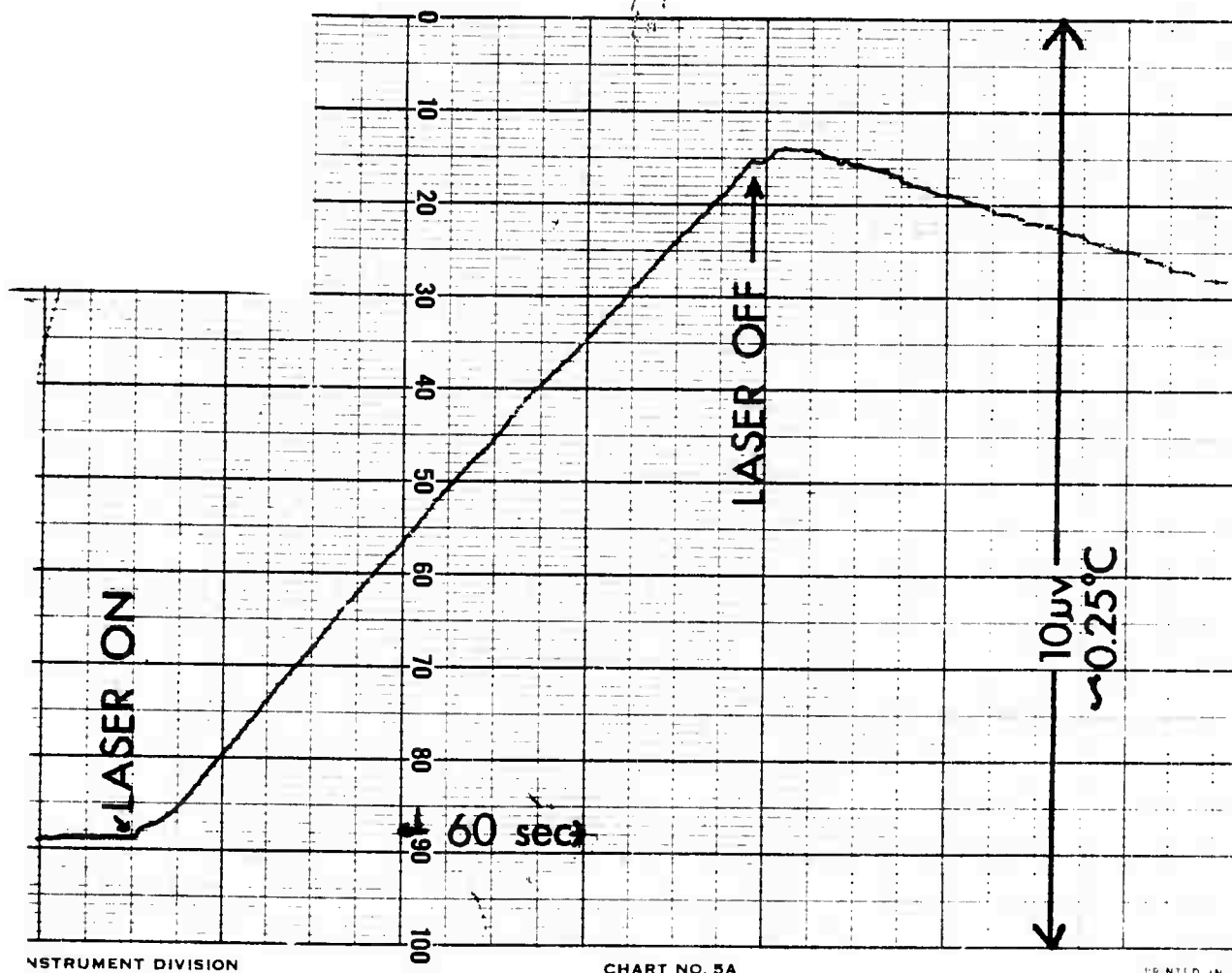


Fig. 2. Heating curve of KCl irradiated with one watt at 10.6 μm .